Gibbs Ensemble Monte Carlo Simulation for Vapor-Liquid Equilibrium of Binary Mixtures CO_2/C_3H_8, CO_2/CH_3OCH_3, and CO_2/CH_3COCH_3

Sung-Doo Moon* **and Byung Kee Moon†**

Department of Chemistry, Pukyong National University, Pusan 608-737, Korea
†Department of Physics, Pukyong National University, Pusan 608-737, Korea
Received July 25, 2000

Gibbs ensemble Monte Carlo simulations were performed to calculate the vapor- liquid coexistence properties for the binary mixtures CO_2/C_3H_8, CO_2/CH_3OCH_3, and CO_2/CH_3COCH_3. For all the molecules the potential between sites in different molecules was simply calculated by the Lennard-Jones potential. Density of the mixture, composition of the mixture, the pressure-composition diagram, the chemical potential of component, and the radial distribution function were calculated at vapor- liquid equilibrium. The composition and the density of both vapor and liquid from simulation agreed considerably well with the experimental values over a wide range of pressures. The radial distribution functions in the liquid mixtures showed that CO_2 molecules tended to form cluster with each other and C_3H_8 molecules also aggregated each other due to the weak interaction between CO_2 and C_3H_8 molecule. However the interaction potentials between the same components were similar to those between the different components in the liquid mixtures CO_2/CH_3OCH_3 and CO_2/CH_3COCH_3.

Introduction

There has been much progress in the development of molecular simulations. Simulation-based techniques can be used to predict the phase behavior of real fluids at conditions for which experimental data are difficult or impossible to obtain, and provide significantly more reliable results than those obtained with approximate theoretical methods, since they eliminate all uncertainties in connecting macroscopic properties to the microscopic characteristics of a system.[1]

The Gibbs ensemble Monte Carlo (GEMC) simulation[2] enables us to calculate the phase equilibrium of pure components and mixtures, and is more convenient than the indirect method involving computations of the chemical potential. GEMC simulation has been used to calculate the equilibrium properties of small molecules, that is, methyl iodide,[3] Lennard-Jones (LJ) fluid,[4] and CO_2/C_2H_6 mixtures.[5] For larger molecules such as chain hydrocarbons, the probability of the successful insertion of a molecule into a high density system in simulations is very low. Therefore a combination of the GEMC simulation with the configurational bias Monte Carlo technique[6] has been used recently. For example, this method has applied to calculate the phase equilibrium of *n*-alkanes,[7] branched alkanes,[8] alkanols,[9] *n*-alkanes mixtures,[10] CO_2/perfluoroalkane mixture,[11] and methanethiol/C_3H_8 mixture.[12]

Supercritical CO_2 has been used as an extraction solvent in many industries. It is nontoxic, nonflammable, and relatively inexpensive.[13] Its low critical temperature is especially suitable for thermally labile materials. The extraction efficiency of supercritical CO_2 can be improved with the addition of cosolvents. Goldman[14] *et al*. reported that increasing the strength of the interaction between solute and cosolvent enhanced the solubility, while increasing the strength of the interaction between solvent and cosolvent increased or decreased the solubility, depending on the operating conditions.

In this study we carried out GEMC simulations to calculate the vapor-liquid coexistence properties for CO_2 mixtures with CP2, which denotes C_3H_8, CH_3OCH_3, and CH_3COCH_3. The calculated properties were compared with the experimental values.

Molecular Model and Simulation Method

For the reasons of simplicity, the two-center Lennard-Jones (2CLJ) model[15] for CO_2 was used, in which the CO_2 molecule was assumed to be composed of two sites connected by a rigid length of 0.237 nm. One of us has performed molecular simulations using the 2CLJ model in the study[16] of CO_2 fluid and obtained thermodynamic properties in fair agreement with experimental values.

For the CP2 molecules, CH_3 and CH_2 groups were considered as single interaction sites, and bond lengths and bond angles were fixed in simulation. The geometries of CP2 molecules were adopted as follows: r(C-C)=0.153 nm and $\angle$ CCC=112° for C_3H_8 molecule,[17] r(C-O)=0.141 nm and $\angle$ COC=112° for CH_3OCH_3 molecule,[18] r(C-C)=0.152 nm, r(C=O)=0.1213 nm, and $\angle$CCC=116° for CH_3COCH_3 molecule.[19]

The potential between sites in different molecules was calculated by LJ potential.

$$u_{ij} = 4\varepsilon_{ij}\left[\left(\frac{\sigma_{ij}}{r_{ij}}\right)^{12} - \left(\frac{\sigma_{ij}}{r_{ij}}\right)^{6}\right] \quad (1)$$

where u_{ij} is the pairwise potential and r_{ij} is the distance between sites i and j. The size parameter σ and the energy parameter ε of CP2 molecules are summarized in Table 1, in which the ε of CH_3 in CH_3OCH_3 and CH_3COCH_3 molecules is about 10% greater than that in C_3H_8 molecule. The small increases of ε's of the sites in CH_3OCH_3 and CH_3COCH_3 molecules compensate for the neglect of the electrostatic

Table 1. Site parameters for propane, dimethyl ether, and acetone

Site	σ (nm)	ε/k (K)
CH_3 (propane)	0.394[a]	90.5[a]
CH_2 (propane)	0.394[a]	49.3[a]
CH_3 (acetone and ether)	0.394[b]	99.55[b]
C (acetone)	0.375[c]	58.19[d]
O (acetone)	0.296[c]	116.27[d]
O (ether)	0.3[c]	94.14[d]

[a]from ref. 7, [b]estimated values, [c]from ref. 20, [d]The values are about 10% greater than those in ref. 20.

energy due to the dipole-dipole interaction.

For each site of CO_2, the value σ=0.2989 nm was taken from the 2CLJ model,[15] but a slightly smaller value of ε was used in this study. The value of ε/k for CO_2 was assumed to be 150.512 K.[16] The potential between CO_2 molecules calculated with these values of ε and σ includes the contribution of potential arising from the quadrupole-quadrupole interaction between CO_2 molecules.

For the LJ interactions between the sites in different molecules, the modified Lorentz-Berthelot rules were used as follows:

$$\sigma_{ij} = 0.5(\sigma_{ii} + \sigma_{jj}) \tag{2}$$

$$\varepsilon_{ij} = (1-\delta_{ij})(\varepsilon_{ii}\varepsilon_{jj})^{0.5} \tag{3}$$

where σ_{ij} is the cross size parameter, ε_{ij} is the cross energy parameter, and δ_{ij} is the inter-site interaction parameter.

Simulation Method. The GEMC simulations were carried out using conventional procedures[2] in principle. All simulations were performed for a total of 512 molecules in the two cubic simulation boxes I and II, and three dimensional periodic boundary conditions were used.

The types of Monte Carlo moves were as follows:

(a) molecule translation. A molecule was selected at random and was displaced in randomly chosen cartesian direction. The trial move was accepted with a probability given by

$$P_m = \min [1, \exp(-\beta\Delta E)] \tag{4}$$

where ΔE is the energy change for the trial move in box I or II, and β is 1/kT. Here k is Boltzmann constant, and T is temperature.

(b) molecule rotation. A molecule was selected at random and was rotated. The center of the rotation was at the center of a molecule, and the molecule was rotated about an axis parallel to a randomly chosen cartesian axis. The trial move was accepted with a probability given by Eq. (4).

(c) volume rearrangement in the NPT ensemble. For random volume changes of simulation boxes I and II, the trial move was accepted with a probability given by

$$P_v = \min[1, \exp(-\beta[\Delta E^{\mathrm{I}} + \Delta E^{\mathrm{II}} - N^{\mathrm{I}}kT\ln\frac{V^{\mathrm{I}} + \Delta V^{\mathrm{I}}}{V^{\mathrm{I}}} - N^{\mathrm{II}}kT\ln\frac{V^{\mathrm{II}} + \Delta V^{\mathrm{II}}}{V^{\mathrm{II}}} + P(\Delta V^{\mathrm{I}} + \Delta V^{\mathrm{II}})])] \tag{5}$$

where P is pressure, ΔV^{I} and ΔV^{II} are the volume changes of simulation box I and II, respectively. In Eq. (5), N^{I} and N^{II} are the number of molecules in box I and II, respectively. A volume change of only one box was attempted at a time in this study. That is, one box was chosen at random and its volume was changed by a random amount.

(d) molecule transfer. It was first decided at random to choose box I or II for the trial creation. Then the type of molecule to be transferred was chosen at random, and finally a random molecule of that type was transferred. For a transfer of a molecule of type i from box II to I, the trial move was accepted with a probability given by

$$P_t = \min[1, \exp(-\beta[\Delta E^{\mathrm{I}}+\Delta E^{\mathrm{II}} + kT\ln\frac{V^{\mathrm{II}}(N_i^{\mathrm{I}} + 1)}{V^{\mathrm{I}}N_i^{\mathrm{II}}}])] \tag{6}$$

where N_i^{I} and N_i^{II} are the number of molecules of type i in box I and II, respectively. If box II is chosen for the creation, the superscripts I and II in Eq. (6) are interchanged.

Each configuration in simulations was generated by a randomly selected Monte Carlo move. The four types of Monte Carlo moves occurred with the following probabilities: 35%, 35%, 10%, and 20% for move (a), (b), (c), and (d), respectively. For move (a), (b), and (c), the maximum move was adjusted to give an average acceptance ratio of 40 % every 25000 configurations. All the interactions were truncated if the inter-site distance was larger than cutoff distance, which was half the length of the simulation box. The corrections to the potential arising from truncations of inter-site interactions were taken into account using the method given by Jorgensen.[21]

The initial configurations were obtained by putting 256 molecules on a face-centered cubic lattice in each of the simulation boxes. The initial densities were taken as 0.1 g/cm^3 for the vapor phase and were taken as 0.5 or 0.8 g/cm^3 for liquid phase. The simulation results were not almost affected by the initial densities. However the initial compositions were chosen to be approximately the experimental compositions of the vapor and the liquid phases for fast equilibration.

Although GEMC simulation does not require knowledge of the chemical potentials, the chemical potential of each component in each simulation box was calculated to test convergence of the simulation. The chemical potential of component i in simulation box j is given by[12]

$$\mu_{ji} = -kT\ln\langle\frac{V_j}{N_{ji}+1}\exp\left(-\frac{U_{ji}^{+}}{kT}\right)\rangle \tag{7}$$

where the symbol $\langle\cdots\rangle$ denotes the ensemble average, V_j is the volume of simulation box j, N_{ji} is the number of molecules of component i in simulation box j, and U_{ji}^{+} is the potential of the test molecule of component i in simulation box j.

The number of configurations generated in equilibration run was 1×10^6 to 1.5×10^6, and that in equilibrium run was 1.5×10^6 to 2.5×10^6. The simulation run was divided into many blocks, each of which consists of 25000 configura-

tions. The properties of the system were calculated by accumulating the properties every 50 configurations and by averaging them. The estimated errors for properties were obtained by calculating the standard deviation of the block average properties.

Results and Discussion

GEMC simulation can be applied from close to the melting point to the vicinity of the critical point. However at conditions so close to the critical point, the fluctuations in density of the two coexisting phases increase and the simulation results depend on the system size.

Table 2 shows the simulation results for some mixtures along with the experimental results. The calculated mole fractions of CO_2 in both vapor and liquid agree considerably well with the experimental values over a wide range of pressures. Especially for the mixtures CO_2/CH_3OCH_3 at 308.5 K, the mole fractions of CO_2 from simulation are average 2.3% larger than the experimental values. The chemical

Table 2. Simulation results for the binary mixtures CO_2 (1)/ CP2(2)[a] (P; pressure, y_1; mole fraction of CO_2 in the vapor, x_1; mole fraction of CO_2 in the liquid, ρ_V; density of the vapor, ρ_L; density of the liquid, μ_{Vi}; chemical potential of component i in the vapor, μ_{Li}; chemical potential of component i in the liquid, R_t; successful transfer of molecule)

P	y_1		x_1		ρ_V	ρ_L	$-\mu_{V1}$	$-\mu_{L1}$	$-\mu_{V2}$	$-\mu_{L2}$	R_t
(MPa)	expl.[b]	simu.	expl.[b]	simu.	(g/cm^3)	(g/cm^3)	(kJ/mol)	(kJ/mol)	(kJ/mol)	(kJ/mol)	(%)
mixture CO_2/C_3H_8 at 244.26 K											
0.752	0.782	0.728(9)	0.225	0.256(14)	0.018(1)	0.579(12)	17.8	17.8	20.0	19.5	0.40
0.920	0.830	0.809(10)	0.323	0.338(16)	0.022(2)	0.605(12)	17.2	17.5	20.4	21.7	0.38
1.064	0.858	0.838(11)	0.423	0.425(17)	0.026(2)	0.630(16)	16.9	17.1	20.5	21.1	0.42
1.158	0.883	0.875(9)	0.533	0.483(23)	0.029(2)	0.650(20)	16.7	16.5	20.8	20.5	0.43
1.272	0.907	0.888(6)	0.667	0.642(21)	0.032(2)	0.723(24)	16.5	16.2	20.9	20.9	0.40
1.358	0.932	0.920(13)	0.807	0.793(20)	0.034(2)	0.798(31)	16.3	16.4	21.5	21.6	0.40
mixture CO_2/C_3H_8 at 266.48 K											
1.069	0.640	0.603(16)	0.162	0.171(22)	0.024(2)	0.522(13)	19.3	19.5	20.5	20.4	0.91
1.362	0.725	0.681(12)	0.252	0.247(24)	0.032(2)	0.541(15)	18.5	18.3	20.6	20.6	0.82
1.662	0.788	0.759(23)	0.346	0.342(21)	0.039(3)	0.570(16)	17.9	17.8	20.8	19.4	0.82
2.027	0.832	0.781(12)	0.443	0.470(19)	0.051(4)	0.604(19)	17.5	17.1	20.7	20.3	0.86
2.420	0.875	0.851(18)	0.647	0.637(23)	0.063(5)	0.661(22)	16.9	17.1	21.3	21.5	0.94
2.613	0.927	0.917(10)	0.819	0.766(38)	0.068(6)	0.698(40)	16.7	16.5	22.4	21.8	1.26
mixture CO_2/CH_3OCH_3 at 273 K											
1.09	0.796	0.801(18)	0.366	0.359(32)	0.024(2)	0.700(18)	19.1	19.5	22.6	21.7	0.31
1.24	0.835	0.843(11)	0.428	0.388(15)	0.027(2)	0.708(18)	18.8	18.8	22.9	21.9	0.30
1.73	0.900	0.893(11)	0.572	0.525(18)	0.040(3)	0.747(18)	17.9	17.8	23.2	21.7	0.31
2.07	0.930	0.918(11)	0.663	0.661(14)	0.049(4)	0.789(20)	17.6	17.1	23.5	25.5	0.36
2.41	0.953	0.938(11)	0.744	0.697(25)	0.059(4)	0.805(21)	17.2	17.1	24.0	23.0	0.33
mixture CO_2/CH_3OCH_3 at 308.5 K											
1.59	0.499	0.523(17)	0.184	0.192(17)	0.033(3)	0.605(14)	22.0	21.8	22.7	22.4	0.84
2.45	0.686	0.703(15)	0.354	0.353(17)	0.053(4)	0.638(19)	20.3	20.0	23.1	23.0	0.85
3.07	0.770	0.782(22)	0.457	0.452(17)	0.070(6)	0.655(19)	19.5	19.4	23.5	22.4	0.99
3.79	0.824	0.841(19)	0.570	0.566(25)	0.090(9)	0.669(26)	18.9	18.8	24.2	23.7	1.21
4.48	0.867	0.864(19)	0.660	0.627(23)	0.115(10)	0.699(23)	18.4	18.5	24.5	24.0	1.03
5.17	0.896	0.907(19)	0.743	0.712(22)	0.143(21)	0.705(33)	18.0	18.0	25.5	24.9	1.35
mixture CO_2/CH_3COCH_3 at 291.15 K											
1.18	0.979	0.971(4)	0.289	0.292(11)	0.023(2)	0.778(11)	19.9	19.8	28.6	26.7	0.08
2.41	0.985	0.978(3)	0.521	0.513(11)	0.052(4)	0.814(15)	18.3	18.5	28.3	28.1	0.11
3.10	0.990	0.992(4)	0.655	0.618(11)	0.069(6)	0.842(17)	17.8	17.5	30.6	32.3	0.15
3.84	0.987	0.995(5)	0.767	0.800(6)	0.093(9)	0.850(16)	17.3	17.3	31.1	32.4	0.36
4.34	0.984	0.996(3)	0.818	0.793(8)	0.113(10)	0.856(21)	17.1	16.8	31.8	30.7	0.32
mixture CO_2/CH_3COCH_3 at 313.13 K											
1.18	0.942	0.923(6)	0.186	0.161(18)	0.022(1)	0.743(9)	21.7	21.9	28.5	29.4	0.10
2.03	0.956	0.953(5)	0.304	0.287(11)	0.039(3)	0.756(12)	20.3	19.8	28.8	26.9	0.14
2.80	0.965	0.967(6)	0.403	0.390(10)	0.056(4)	0.769(15)	19.5	19.0	29.3	31.4	0.17
4.60	0.986	0.977(4)	0.619	0.639(7)	0.104(9)	0.801(19)	18.4	18.4	29.9	31.3	0.32

[a]The numbers in parentheses indicate the uncertainty in units of the last decimal digit. [b]The experimental data were obtained from ref. 22, ref. 23, and ref. 24 for mixtures CO_2/C_3H_8, CO_2/CH_3OCH_3, and CO_2/CH_3COCH_3, respectively.

potentials of CO_2 in the vapor are closely equal to those in the liquid. But the chemical potentials of CP2 in the vapor are somewhat different from those in the liquid, which indicates that the molecule transfer is not efficient. The values of the successful transfers range from 0.08% to 1.35% as shown in Table 2. To increase the acceptance ratio of the molecule transfer, Panagiotopoulos[25] has proposed the particle-identity exchange method, in which a small molecule in one phase exchanges identity with a large molecule in the coexisting phase. However the disadvantage of the method is that the probability of successful exchange of molecules is very low if the difference in the molecular sizes of components is much large.

Estimating the value of δ_{ij} is difficult because thermodynamic properties are significantly sensitive to the interaction potentials. For interactions between CO_2 and CP2, the values of δ_{ij} were determined from fitting to the vapor-liquid equilibrium data[22-24] for binary mixtures in this study. The values of δ_{ij} were set at 0.1, 0, and 0 for CO_2-C_3H_8, CO_2-CH_3OCH_3, and CO_2-CH_3COCH_3, respectively. The values of ε_{ij} for CO_2-C_3H_8 are somewhat smaller than those predicted by the normal mixing rules. This may be mainly due to the fact that the interaction of the quadrupole-quadrupole does not exist between CO_2 and C_3H_8.

Figure 1, 2, and 3 show the pressure-composition diagram for the binary mixtures CO_2/C_3H_8, CO_2/CH_3OCH_3, and CO_2/CH_3COCH_3, respectively. In the vapor of the mixture CO_2/C_3H_8, the mole fractions of CO_2 from simulation are generally smaller than the corresponding experimental values. The largest deviation is from the vapor mixture at 244.26 K and 0.752 MPa, where the mole fraction of CO_2 from simulation is about 7% smaller than the experimental value.

The experimental densities and the calculated densities of the mixture CO_2/CH_3COCH_3 at vapor-liquid equilibrium are shown in Figure 4. The simulation results agree fairly well with the experimental ones. We were not able to find the experimental vapor-liquid coexistence density of the mixtures CO_2/C_3H_8 and CO_2/CH_3OCH_3 with which to compare our coexistence density from simulation.

Figure 5 shows the radial distribution function (RDF) of CO_2-CO_2, CO_2-CP2, and CP2-CP2 in the liquid mixtures. For the same mixtures, the shapes of the RDF's are nearly independent of the concentration and temperature but are

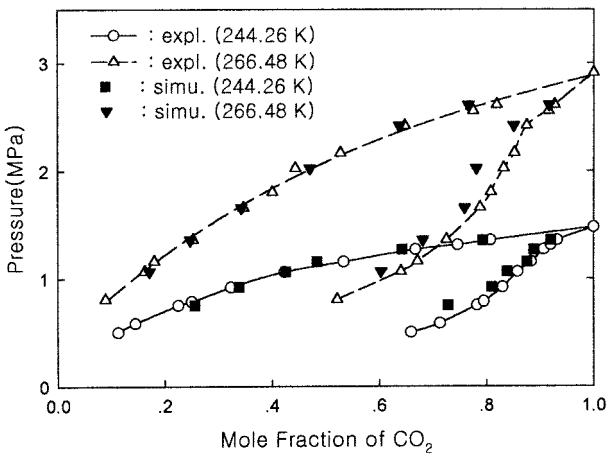

Figure 1. The pressure-composition diagram for the binary mixtures CO_2/C_3H_8. Experimental data were taken from ref. 22.

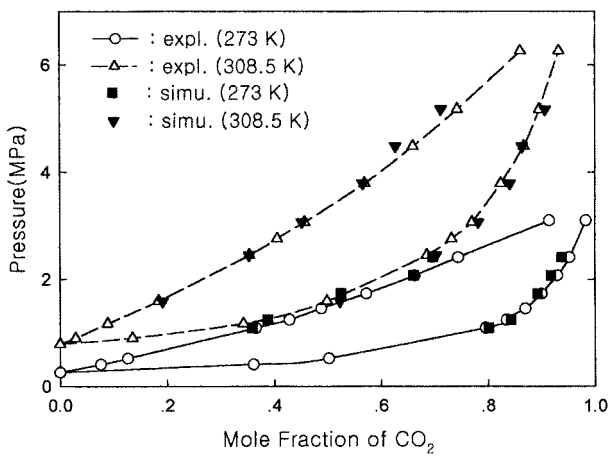

Figure 2. The pressure-composition diagram for the binary mixtures CO_2/CH_3OCH_3. Experimental data were taken from ref. 23.

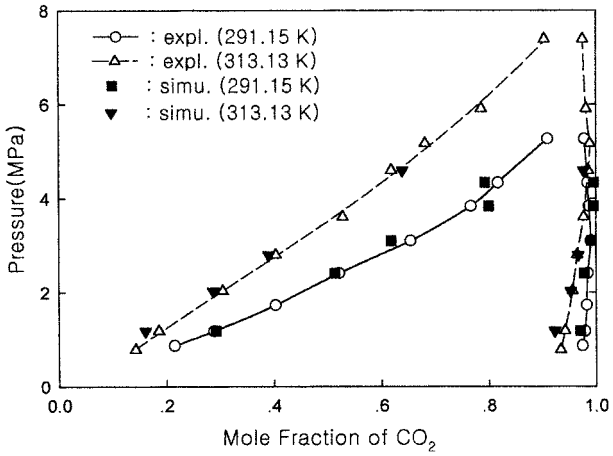

Figure 3. The pressure-composition diagram for the binary mixtures CO_2/CH_3COCH_3. Experimental data were taken from ref. 24.

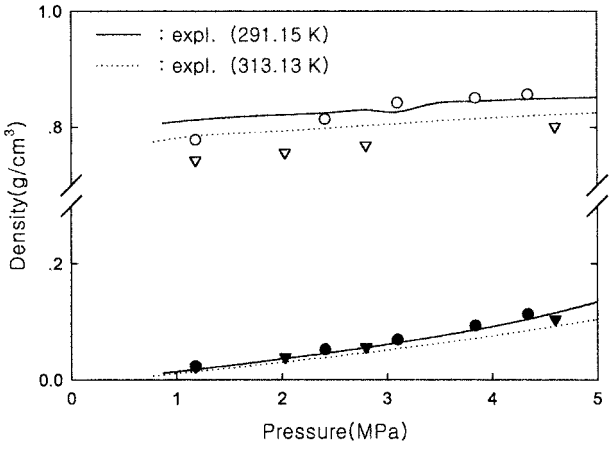

Figure 4. Simulated densities of the vapor and the liquid for the mixtures CO_2/CH_3COCH_3 at 291.15 K (●, ○) and 313.13 K (▼, ▽). Experimental data were taken from ref. 24.

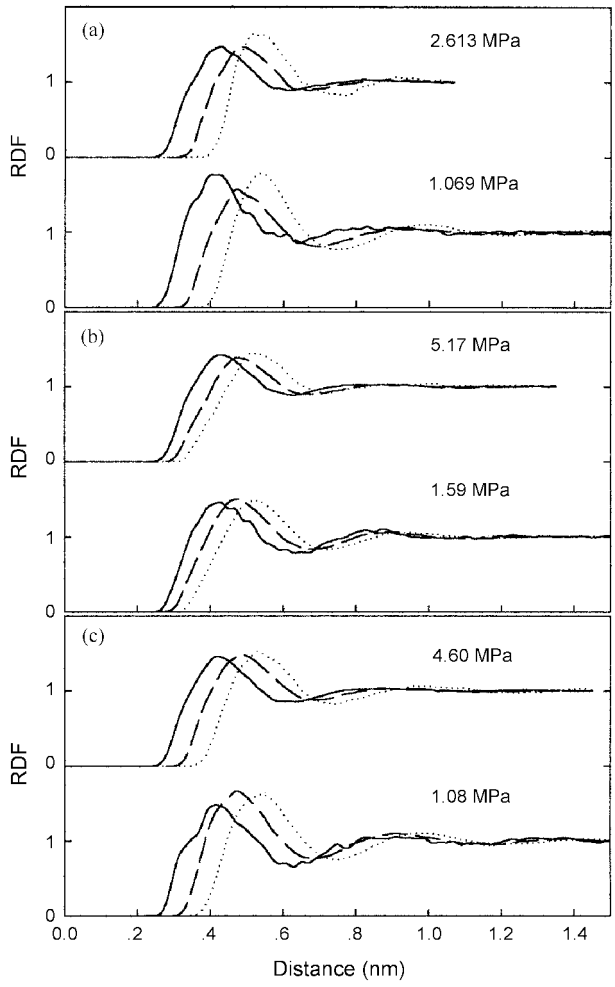

Figure 5. Radial Distribution Function (RDF) in the liquid mixtures (a) CO_2/C_3H_8 at 266.48 K, (b) CO_2/CH_3OCH_3 at 308.5 K, and (c) CO_2/CH_3COCH_3 at 313.13 K; ——: CO_2-CO_2, -----: CP2-CP2, and – – –: CO_2-CP2.

affected by pressure in this study. Figure 5 shows that all the first peaks in mixture at lower pressure are higher than those at higher pressure for the same mixtures, and the second peaks in mixture at higher pressure no longer appear. This means that the liquid is somewhat less structured at higher pressure. Figure 5(a) shows that the first peaks of CO_2-CO_2 and C_3H_8-C_3H_8 are larger and much higher than those of CO_2-C_3H_8. This indicates that CO_2 molecules tend to form cluster with each other and C_3H_8 molecules also aggregate each other due to the weak interaction between CO_2 and C_3H_8 molecule. On the other hand, the heights of the first peaks in Figure 5(b) are nearly the same as well as those in Figure 5(c), which suggests that the interaction potential of CO_2-CP2 is similar to those of CO_2-CO_2 and CP2-CP2 in the mixtures CO_2/CH_3OCH_3 and CO_2/CH_3COCH_3.

Acknowledgment. The authors acknowledge the use of the IBM SP2 computer in the Tongmyung University of Information Technology.

References

1. Panagiotopoulos, A. Z. *Mol. Simulation* **1992**, *9*, 1.
2. Panagiotopoulos, A. Z.; Quirke, N.; Stapleton, M.; Tildesley, D. J. *Mol. Phys.* **1988**, *63*, 527.
3. Freitas, F. F. M.; Fernandes, F. M. S. S.; Cabral, B. J. C. *J. Phys. Chem.* **1995**, *99*, 5180.
4. Smit, B. *J. Chem. Phys.* **1992**, *96*, 8639.
5. Liu, A.; Beck, T. L. *J. Phys. Chem. B* **1998**, *102*, 7627.
6. Smit, B.; Siepmann, J. I. *J. Phys. Chem*. **1994**, *98*, 8442.
7. Smit, B.; Karaborni, S.; Siepmann, J. I. *J. Chem. Phys*. **1995**, *102*, 2126.
8. Siepmann, J. I.; Martin, M. G.; Mundy, C. J.; Klein, M. L. *Mol. Phys.* **1997**, *90*, 687.
9. van Leeuwen, M. E. *Mol. Phys.* **1996**, *87*, 87.
10. Martin, M. G.; Siepmann, J. I. *J. Am. Chem. Soc.* **1997**, *119*, 8921.
11. Cui, S. T.; Cochran, H. D.; Cummings, P. T. *J. Phys. Chem. B* **1999**, *103*, 4485.
12. Agrawal, R.; Wallis, E. P. *Fluid Phase Equilibria* **1997**, *131*, 51.
13. Chang, H.; Morrell, D. G. *J. Chem. Eng. Data* **1985**, *30*, 74.
14. Goldman, S.; Gray, C. G.; Li, W.; Tomberli, B.; Joslin, C. G. *J. Phys. Chem.* **1996**, *100*, 7246.
15. Murthy, C. S.; Singer, K. *Mol. Phys*. **1981**, *44*, 135.
16. Moon, S. D. *Bull. Korean Chem. Soc.* **1999**, *20*, 459.
17. de Pablo, J. J.; Laso, M.; Sute, U. W. *J. Chem. Phys*. **1992**, *96*, 2395.
18. Jorgensen, W. L. *J. Am. Chem. Soc*. **1981**, *103*, 335.
19. *Handbook of Chemistry and Physics*, 80th ed.; The Chemical Rubber Co.: Boca Raton, 1999; p 9-24.
20. Carlson, H. A.; Nguyen, T. B.; Orozco, M.; Jorgensen, W. L. *J. Comp. Chem*. **1993**, *14*, 1240.
21. Jorgensen, W. L.; Madura, J. D.; Swenson, C. J. *J. Am. Chem. Soc*. **1984**, *106*, 6638.
22. Hamam, S. E. M.; Lu, B. C. Y. *J. Chem. Eng. Data* **1976**, *21*, 200.
23. Tsang, C. Y.; Streett, W. B. *J. Chem. Eng. Data* **1981**, *26*, 155.
24. Day, C. Y.; Chang, C. J.; Chen, C. Y. *J. Chem. Eng. Data* **1999**, *44*, 365.
25. Panagiotopoulos, A. Z. *Int. J. Thermophys.* **1989**, *10*, 447.